Available online at www.sciencedirect.com

ScienceDirect

Procedia Engineering 124 (2015) 330 – 342

Procedia Engineering

www.elsevier.com/locate/procedia

24th International Meshing Roundtable (IMR24)

Voronoi-based point-placement for three-dimensional Delaunay-refinement

Darren Engwirda[a,b,*]

[a]*Department of Earth, Atmospheric and Planetary Sciences, Massachusetts Institute of Technology, 54-918, 77 Massachusetts Avenue, Cambridge, MA 02139-4307, USA*

[b]*School of Mathematics and Statistics F07, University of Sydney, NSW 2006, Australia*

Abstract

An extension of the restricted Delaunay-refinement algorithm for three-dimensional tetrahedral mesh generation is described, in which an *off-centre* type point-placement scheme is utilised. It is shown that the use of generalised Steiner points, positioned along edges in the associated Voronoi complex, typically leads to improvements in the overall size, quality and grading of the resulting tetrahedral meshes. The new algorithm can be viewed as a Frontal-Delaunay approach – a hybridisation of conventional Delaunay-refinement and advancing-front techniques, in which new vertices are positioned to satisfy both element size- and shape-constraints. The new method is shown to inherit many of the best features of classical Delaunay-refinement and advancing-front type algorithms, combining good practical performance with theoretical robustness. Experimental comparisons show that the new method outperforms classical Delaunay-refinement techniques for a number of three-dimensional benchmark problems.

Peer-review under responsibility of organizing committee of the 24th International Meshing Roundtable (IMR24)

Keywords: Three-dimensional mesh generation, Delaunay-refinement, Advancing-front, Frontal-Delaunay, Off-centres

1. Introduction

Three-dimensional mesh generation is a key component in a variety of computational modelling and simulation tasks, including problems in computational engineering, numerical modelling, computer graphics and animation. Given a general volumetric domain, described by a piecewise smooth surface $\Sigma \subset \mathbb{R}^3$ enclosing a volume Ω, the tetrahedral meshing problem consists of tessellating both Σ and Ω into a *mesh* of non-overlapping triangular and tetrahedral elements, such that all geometrical, topological and user-defined constraints are satisfied. It is typical to require that such tessellations: (i) are conforming – ensuring that the triangulation of Σ is embedded within the tessellation of Ω, (ii) include elements of high shape-quality, (iii) provide good geometrical and topological approximations to the underlying surface Σ and volume Ω, and (iv) satisfy a set of user-specified sizing constraints. While various strategies have been presented to solve this problem in the past, a new algorithm is developed in this study with the aim of improving the quality of the resulting tessellations. This new tetrahedral refinement algorithm is an extension of the

* Corresponding author. Tel.: +1-212-678-5521.
E-mail address: engwirda@mit.edu

Peer-review under responsibility of organizing committee of the 24th International Meshing Roundtable (IMR24)
doi:10.1016/j.proeng.2015.10.143

restricted Frontal-Delaunay surface meshing algorithm presented by the author in [1,2] to support the generation of quality tetrahedral meshes in bounded volumetric domains.

1.1. Related work

Three-dimensional mesh generation is a broad and evolving area of research. Many successful algorithms employ one of two approaches: (i) an *advancing-front* technique [3–6], in which meshes are generated by incrementally positioning new vertices and elements adjacent to a set of *frontal-facets*, or (ii) a *Delaunay-based* strategy [7–16], based on the progressive refinement of a coarse initial Delaunay triangulation.

Delaunay-refinement schemes are *top-down* algorithms – based on the incremental *refinement* of a bounding Delaunay tessellation. At each step of the algorithm, elements that violate a set of constraints are identified and the worst offending elements are *eliminated*. Elimination is achieved through the insertion of additional *Steiner-vertices* located at the refinement points of the associated elements. The original two-dimensional Delaunay-refinement methods of Chew [7] and Ruppert [8,9] have since given rise to methods for fully three-dimensional refinement [11] and the refinement of embedded surfaces [14,15]. This study is focused on use of the so-called *restricted* Delaunay-refinement method [13,16,17] which provides a framework for the approximation of volumetric domains via Delaunay sub-complexes. It has been shown [13–15,18] that if the domain is sampled in a *sufficiently-dense* and *well-distributed* fashion, the restricted Delaunay sub-complexes offer an accurate piecewise approximation of the volume Ω and its bounding surface Σ, incorporating guarantees of geometrical and topological fidelity. One of the key advantages of a restricted Delaunay refinement approach is that the surface and volume of the domain are sampled in a unified manner [16] – obviating non-trivial difficulties associated with the construction of constrained tetrahedral complexes conforming to a given set of surface constraints [19,20].

Advancing-front schemes, in contrast, are *bottom-up* algorithms – constructing meshes in a *local* fashion through the incremental addition of new vertices and elements adjacent to a set of *frontal-facets*. Unlike Delaunay-based methods, which maintain a tessellation of the full domain throughout, frontal schemes seek to assemble the full tessellation progressively – with new elements inserted to gradually 'fill-in' the interior of the domain. In three-dimensions, such a process is known to be non-robust, due to the existence of polyhedral cavities that do not support conforming tetrahedralisations. Nonetheless, it is known that when optimised advancing-front schemes do converge, they often produce tessellations of significantly improved quality compared to Delaunay-based methods [4,5].

In this study, a new *Frontal-Delaunay* algorithm is presented which seeks to combine the benefits of classical Delaunay-refinement and advancing-front type approaches. The new algorithm is designed to produce smooth, high-quality triangulations consistent with advancing-front type schemes, whilst also inheriting the theoretical robustness of Delaunay-based techniques. It is expected that this new algorithm may be of interest to users who place a high premium on mesh quality, including those operating in the areas of computational engineering and numerical simulation.

An overview of an existing state-of-the-art restricted Delaunay-refinement scheme is presented in Section 2. The new Frontal-Delaunay algorithm is presented in Section 3, focusing in-detail on the new *off-centre* point-placement schemes for both surface- and volume-based refinement operations. In Section 6, an experimental comparison between the conventional Delaunay-refinement and the proposed Frontal-Delaunay schemes is presented, contrasting output quality and computational performance.

2. Restricted Delaunay-refinement techniques

Three-dimensional restricted Delaunay-refinement algorithms operate by incrementally introducing new Steiner vertices into an initially coarse Delaunay tessellation of the volume to be meshed. Such methods typically also seek to build a high-quality triangulation of the bounding surface of the domain, *embedded* within the volumetric complex. Contrary to typical planar algorithms [7–9], such refinement schemes are designed not only to ensure that the resulting mesh satisfies element shape- and size-constraints, but that the geometry and topology of the mesh itself is an accurate piecewise approximation to both the volumetric domain Ω and its bounding surface Σ.

The meshing algorithms presented in this study are based on the so-called *restricted* Delaunay surface and volume tessellations $\mathrm{Del}|_\Sigma(X)$ and $\mathrm{Del}|_\Omega(X)$ – triangular and tetrahedral sub-complexes of the full-dimensional Delaunay tessellation $\mathrm{Del}(X)$. Specifically, the restricted surface triangulation $\mathrm{Del}|_\Sigma(X) \subseteq \mathrm{Del}(X)$ contains the set of 2-simplexes

Fig. 1. Restricted tessellations for a curved domain in $\mathbb{R}^2$, showing (i) the curve Σ and enclosed area Ω, (ii) the Delaunay tessellation Del(X) and Voronoi diagram Vor(X), and (iii) the restricted curve and area tessellations Del $|_\Sigma(X)$ and Del $|_\Omega(X)$. In three-dimensions, the restricted surface triangulation Del $|_\Sigma(X)$ is a triangular complex that covers the surface Σ. The restricted volume tessellation Del $|_\Omega(X)$ is a tetrahedral complex that fills the volume Ω.

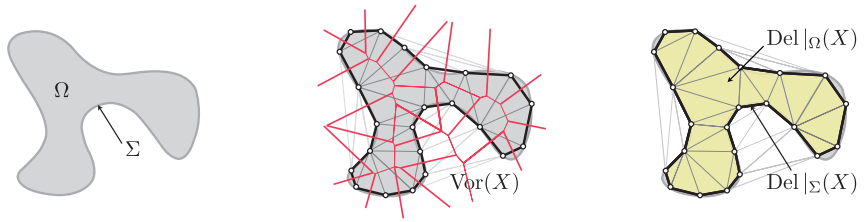

that approximate the bounding surface Σ, while the restricted volume tessellation Del $|_\Omega(X) \subseteq$ Del(X) contains the set of 3-simplexes approximating the volumetric domain Ω. An extensive overview of these concepts is provided in [13,16,18]. In this study, the following formalism is used throughout:

Nomenclature

Ω	The input domain – a bounded volume in $\mathbb{R}^3$ (See Figure 1(i));
Σ	The bounding surface $\Sigma = \partial\Omega$ (See Figure 1(i));
X	The current set of points added to the tessellation;
Del(X)	The Delaunay triangulation of the points X;
Vor(X)	The Voronoi complex associated with the points X;
Del $|_\Sigma(X)$	A sub-complex of the Delaunay tessellation Del(X), *restricted* to the surface Σ. Del $|_\Sigma(X)$ contains the set of 2-simplexes $f \in$ Del(X) whose dual Voronoi edges $v_e \in$ Vor(X) intersect the surface Σ (See Figure 1(ii)–1(iii));
Del $|_\Omega(X)$	A sub-complex of the Delaunay tessellation Del(X), *restricted* to the volume Ω. Del $|_\Omega(X)$ contains the set of 3-simplexes $\tau \in$ Del(X) whose dual Voronoi vertices (circumcentres) $v_p \in$ Vor(X) lie within the volume Ω (See Figure 1(ii)–1(iii));
SDB(f)	The surface Delaunay ball $B(\mathbf{c}, r)$ associated with a 2-simplex $f \in$ Del $|_\Sigma(X)$. Surface balls are centred at intersections between the associated bipolar Voronoi edge $v_e \in$ Vor(X) and the surface Σ, such that $\mathbf{c} = v_e \cap \Sigma$ (See Figure 2);
$\rho(\tau)$	The radius-edge ratio for a simplex τ. Defined as the ratio of the radius of the circumball of τ to its shortest edge;
$\epsilon(f)$	The surface discretisation error associated with a 2-simplex $f \in$ Del $|_\Sigma(X)$. Defined as the length from the centre of SDB(f) to the centre of the diametric ball of f (See Figure 2(ii));
$\bar{h}(\mathbf{x})$	The mesh size function. A function $f(\mathbf{x}) : \mathbb{R}^3 \to \mathbb{R}^+$ defining the desired edge length at all points $\mathbf{x} \in \Omega$;
$\nu(\tau)$	The volume-length ratio associated with a given element τ. Defined as $\nu(\tau) = V/\|\mathbf{e}\|^3_{\text{rms}}$, where V is the signed volume of τ and $\|\mathbf{e}\|_{\text{rms}}$ is the root-mean-square edge length. The volume-length ratio is a *robust* measure of element quality.

The reader is referred to [18] for formal definitions and discussions.

2.1. An existing algorithm

The development of provably-good restricted Delaunay-refinement schemes for three-dimensional mesh generation is an ongoing area of research. An algorithm for the meshing of volumes enclosed by smooth 2-manifold surfaces

Fig. 2. The surface Delaunay ball (SDB) for a restricted 2-face $f \in \mathrm{Del}\,|_\Sigma(X)$, showing (i) placement of the surface ball at the intersection of the associated dual edge $\mathbf{v}_f \in \mathrm{Vor}(X)$ and the surface Σ, and (ii) associated SDB radius $r(f)$ and surface discretisation error $\epsilon(f)$.

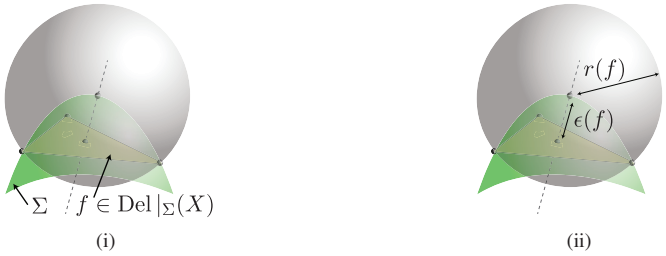

embedded in $\mathbb{R}^3$ is presented here, adapted largely from the methods presented by Cheng, Dey and Shewchuk in [18], which expand on previous techniques due to Cheng, Dey and Levine [21]. Oudot, Rineaua and Yvinec present similar algorithms in [22]. This method is largely equivalent to that of the `CGALMESH` algorithm, available as part of the `CGAL` package, and summarised by Jamin, Alliez, Yvinec and Boissonnat in [16]. The algorithm presented in this section is referred to as the *conventional* Delaunay-refinement approach, due to its direct use of circumcentre-based point-placement schemes.

As per Jamin et al. [16], the development of the conventional Delaunay-refinement algorithm is *geometry-agnostic*, being independent of the specific representation used for the underlying geometry Ω. It is required only that the geometry support a so-called *oracle* predicate that can be used to (i) compute the intersection of a given line segment with the surface Σ, and (ii) determine whether a given point $\mathbf{p}$ lies within the volume Ω. The Frontal-Delaunay algorithm presented in Section 3, additionally requires that the oracle compute intersections between a disk of a given radius and the surface Σ. Such constructions will be discussed in further detail in Section 3. While a broad class of geometry descriptions are supported at the theoretical level, in this study attention is restricted to the development of so-called *remeshing* operations, in which the domains Ω are specified in terms of bounding 2-manifold triangular complexes $\mathcal{P}$. This restriction is made for convenience only – facilitating the construction of simple oracle predicates. Future work is intended to focus on more general descriptions, including domains defined by implicit and analytic functions, in addition to those that contain sharp features.

Following Jamin et al. [16], the Delaunay-refinement algorithm takes as input a volumetric domain Ω, described by an enclosing 2-manifold surface $\Sigma \subseteq \mathbb{R}^3$, an upper bound on the allowable element radius-edge ratio $\bar{\rho}$, a mesh size function $\bar{h}(\mathbf{x})$ defined at all points enclosed by the surface Σ and an upper bound on the allowable surface discretisation error $\bar{\epsilon}(\mathbf{x})$. The algorithm returns a triangulation $\mathcal{T}|_\Sigma$ of the surface Σ, where $\mathcal{T}|_\Sigma$ is a restricted Delaunay surface triangulation of a point-wise sampling $X \in \Sigma$, such that $\mathcal{T}|_\Sigma = \mathrm{Del}\,|_\Sigma(X)$. Additionally, the algorithm also returns a triangulation $\mathcal{T}|_\Omega$ of the enclosed volume Ω, where $\mathcal{T}|_\Omega$ is a restricted Delaunay volumetric triangulation $\mathcal{T}|_\Omega = \mathrm{Del}\,|_\Omega(X)$. Both $\mathrm{Del}\,|_\Sigma(X)$ and $\mathrm{Del}\,|_\Omega(X)$ are sub-complexes of the full-dimensional Delaunay tessellation $\mathrm{Del}(X)$. Note that $\mathrm{Del}\,|_\Sigma(X)$ is a triangular complex, while $\mathrm{Del}\,|_\Omega(X)$ and $\mathrm{Del}(X)$ are tetrahedral complexes. The Delaunay-refinement algorithm is summarised in Algorithm 2.1.

Cheng, Dey and Shewchuk [18] have analysed a similar restricted Delaunay-refinement algorithm and have shown that it guarantees: (i) that all elements in the volumetric tessellation $\tau \in \mathcal{T}|_\Omega$ satisfy constraints on both the element shape and size, such that $\rho(\tau) \leq \bar{\rho}$, and $h(\tau) \leq \bar{h}(\mathbf{x}_\tau)$, (ii) that all elements in the embedded surface triangulation $f \in \mathcal{T}|_\Sigma$ are guaranteed to satisfy similar element shape and size constraints in addition to an upper bound on the allowable surface discretisation error, such that $\epsilon(f) \leq \bar{\epsilon}(\mathbf{x}_f)$, and (iii) that the surface triangulation is *topologically-consistent*, ensuring that $\mathrm{Del}\,|_\Sigma(X)$ is uniformly 2-manifold. Making use of properties of the restricted Delaunay tessellation [17], it is also known that the triangulations $\mathcal{T}|_\Sigma$ and $\mathcal{T}|_\Omega$ are good piecewise linear approximations to the bounding surface Σ and volume Ω, provided that the magnitude of the mesh size function $\bar{h}(\mathbf{x})$ is sufficiently small. Under such conditions it is known that the triangulations $\mathcal{T}|_\Sigma$ and $\mathcal{T}|_\Omega$ are homeomorphic to the underlying surface and volume definitions Σ and Ω, and that the geometric properties of $\mathcal{T}|_\Sigma$ and $\mathcal{T}|_\Omega$ converge toward the true normals, curvature, area and volume of the surface Σ and volume Ω as $\bar{h}(\mathbf{x}) \to 0$.

The Delaunay-refinement algorithm begins by creating an initial point-wise sampling of the surface $X \in \Sigma$. Exploiting the discrete representation available for Σ, the initial sampling is obtained in this study as a *well-distributed*

subset of the existing vertices $Y \in \mathcal{P}$, where $\mathcal{P}$ is the polyhedral representation of the surface Σ. In the next step, the initial triangulation objects are formed. In this study, the full-dimensional Delaunay tessellation, $\mathrm{Del}(X)$, is built using an incremental Delaunay triangulation algorithm, based on the Bowyer-Watson technique [23]. The restricted surface and volumetric triangulations, $\mathrm{Del}\,|_\Sigma(X)$ and $\mathrm{Del}\,|_\Omega(X)$, are derived from $\mathrm{Del}(X)$ by explicitly testing for intersections between the associated Voronoi diagram $\mathrm{Vor}(X)$ and the surface Σ. These queries are computed efficiently by storing the surface definition $\mathcal{P}$ in an AABB-tree [24]. The main loop of the algorithm proceeds to incrementally refine any 2- or 3-simplexes found to be in violation of one or more constraints. Specifically, in step 3, any 2-simplex found to violate the set of radius-edge, mesh-size or surface-error constraints is refined – through the introduction of a new Steiner point $\mathbf{c}_f$ located at the centre of its surface ball $B(\mathbf{c}_f, r)$. In step 4, the topological consistency of the surface triangulation is enforced, ensuring that the set of 2-simplexes $F_p \in \mathrm{Del}\,|_\Sigma(X)$ adjacent to each vertex $\mathbf{p} \in X$ forms a locally 2-manifold surface, known as a *topological-disk*. Vertices adjacent to non-manifold connections trigger additional refinement, with the centres $\mathbf{c}_f$ of the largest adjacent surface balls $B(\mathbf{c}_f, r)$ associated with the triangles $f \in F_p$ inserted as new Steiner points.

Following the initial refinement of the surface triangulation, elements in the volume tessellation $\mathrm{Del}\,|_\Omega(X)$ are refined. In step 5, any 3-simplex found to violate the set of radius-edge or mesh-size constraints is conditionally refined – through the introduction of a new Steiner vertex $\mathbf{c}_\tau$ located at its circumcentre. The insertion of $\mathbf{c}_\tau$ is dependent on several additional constraints. Firstly, in step 5a, if $\mathbf{c}_\tau$ is found to lie within the surface ball $B(\mathbf{c}_f, r)$ of an existing surface facet, that facet is instead refined, through the insertion of a Steiner point located at the centre of its surface ball $\mathbf{c}_f$. This process is similar to the standard edge-encroachment scheme used in Ruppert's two-dimensional refinement algorithm. Secondly, in step 5b, if the insertion of $\mathbf{c}_\tau$ is found to modify the restricted triangulation $\mathrm{Del}\,|_\Sigma(X)$, the insertion is deferred onto an adjacent surface facet. Specifically, the point $\mathbf{c}_\tau$ is deleted from $\mathrm{Del}(X)$ and a new Steiner vertex $\mathbf{c}_f$, corresponding to the centre of the largest adjacent surface ball, is inserted instead. This process ensures that elements in the surface triangulation $\mathrm{Del}\,|_\Sigma(X)$ remain unconnected to interior vertices $\mathbf{p} \neq \Sigma$.

The incremental refinement process continues until all radius-edge, mesh-size, surface-error and topological constraints are satisfied for all elements in both $\mathrm{Del}\,|_\Sigma(X)$ and $\mathrm{Del}\,|_\Omega(X)$. The refinement process is priority scheduled, with triangles $f \in \mathrm{Del}\,|_\Sigma(X)$ and tetrahedrons $\tau \in \mathrm{Del}\,|_\Omega(X)$ ordered according to their radius-edge ratios $\rho(f)$ and $\rho(\tau)$, ensuring that the element with the *worst* ratio is refined at each iteration. Mesh-size constraints are applied with respect to the circumscribing balls associated with each element. Specifically, the mean element sizes $h(f) = \sqrt{3}r_f$ and $h(\tau) = \sqrt{8/3}r_\tau$ are used throughout, where $h(f)$ and $h(\tau)$ denote the size associated with triangles and tetrahedrons respectively. The scalar coefficients represent mappings between circumball radii and edge length for equilateral elements. In this study, mesh-size constraints are implemented as $h(f) \leq \alpha\bar{h}(\mathbf{x}_f)$ and $h(\tau) \leq \alpha\bar{h}(\mathbf{x}_\tau)$, where $\alpha = 4/3$ is a constant factor designed to ensure that the mean element size does not, on average, undershoot the desired target size. The mesh-size functions $\bar{h}(\mathbf{x}_f)$ and $\bar{h}(\mathbf{x}_f)$ are evaluated at the centres of the associated element circumballs.

3. Restricted Frontal-Delaunay Methods

Frontal-Delaunay algorithms are a hybridisation of advancing-front and Delaunay-refinement techniques, in which a Delaunay triangulation is used to define the topology of a mesh while new Steiner vertices are inserted in a manner consistent with advancing-front methodologies. In practice, such techniques have been observed to produce very high-quality meshes, inheriting the smooth, semi-structured vertex placement of pure advancing-front methods and the optimal mesh topology of Delaunay-based approaches. Extending the development of Frontal-Delaunay type methods due to, for example, Üngör and Erten [25], Rebay [26], Mavriplis [27], Frey, Borouchaki and George [28], and Remacle et al. [29], the new algorithm presented in this study is based on a combination of advancing-front and Delaunay-type point-placement rules. This strategy is designed to leverage the improved quality of advancing-front type approaches while preserving the theoretical robustness and guarantees associated with the Delaunay-refinement algorithm presented in Section 2.

3.1. Off-centres

The new Frontal-Delaunay algorithm is based primarily on ideas introduced by Rebay, who, in [26], developed a two-dimensional Frontal-Delaunay algorithm in which new vertices are positioned along edges of the associated

Algorithm 2.1 Three-dimensional restricted Delaunay-refinement

function DelaunayVolume($\Sigma, \Omega, \bar{\rho}, \bar{\epsilon}(\mathbf{x}), \bar{h}(\mathbf{x}), \mathcal{T}|_\Sigma, \mathcal{T}|_\Omega$)
  Form an initial point-wise sampling $X \in \Sigma$ such that X is *well-distributed* on Σ. Compute the Delaunay tessellation Del(X) and the restricted surface and volume tessellations Del$|_\Sigma(X)$ and Del$|_\Omega(X)$.
  If some 2-simplex $f \in$ Del$|_\Sigma(X)$ violates BadSimplex2(f), form the Steiner point $\mathbf{c}_f$ associated with f, insert $\mathbf{c}_f$ into X, update the tessellations Del(X), Del$|_\Sigma(X)$ and Del$|_\Omega(X)$ and go to step 3.
  For all vertices $p \in X$ compute $\mathbf{c}_p \leftarrow$TopoDisk(p). If $\mathbf{c}$ is non-null, insert $\mathbf{c}_p$ into X, update the tessellations Del(X), Del$|_\Sigma(X)$ and Del$|_\Omega(X)$ and go to step 3.
  If some 3-simplex $\tau \in$ Del$|_\Omega(X)$ violates BadSimplex3(τ), form the Steiner point $\mathbf{c}_\tau$ associated with τ.
    (a) If the point $\mathbf{c}_\tau$ lies within a surface ball $B(\mathbf{c}_f, r)$ associated with some 2-face $f \in$ Del$|_\Sigma(X)$, insert $\mathbf{c}_f$ into X instead, update the tessellations Del(X), Del$|_\Sigma(X)$ and Del$|_\Omega(X)$ and go to step 3.
    (b) Insert $\mathbf{c}_\tau$ into X. If $\mathbf{c}_\tau$ changes the surface triangulation Del$|_\Sigma(X)$, such that $\mathbf{c}_\tau \in f$ for some Del$|_\Sigma(X)$, find the largest adjacent surface ball $B(\mathbf{c}_f, r)$, delete $\mathbf{c}_\tau$ from X and insert $\mathbf{c}_f$ into X. Update the tessellations Del(X), Del$|_\Sigma(X)$ and Del$|_\Omega(X)$ and go to step 3.
    (c) Go to step 5.
  Return the restricted Delaunay surface and volume tessellations Del$|_\Sigma(X)$ and Del$|_\Omega(X)$.
end function

function TopoDisk($\mathbf{p}$) ▷ {topological disk about $\mathbf{p}$}
  Find the set of 2-simplexes $F_p \in$ Del$|_\Sigma(X)$ adjacent to the vertex $\mathbf{p}$.
  If F_p is empty or a topological disk, return null.
  Otherwise, find the 2-simplex $f \in F_p$ that maximises the size of the associated surface Delaunay ball $B(\mathbf{c}_f, r)$. Return $\mathbf{c}_f$.
end function

function BadSimplex2(f) ▷ {termination criteria}
  return $(\rho(f) > \bar{\rho})$ or $(\epsilon(f) > \bar{\epsilon}(\mathbf{x}_f))$ or $(h(f) > \bar{h}(\mathbf{x}_f))$
end function

function BadSimplex3(τ) ▷ {termination criteria}
  return $(\rho(\tau) > \bar{\rho})$ or $(h(\tau) > \bar{h}(\mathbf{x}_\tau))$
end function

Voronoi diagram. Rebay showed that new vertices can be positioned on Vor(X) according to a mesh size function $\bar{h}(\mathbf{x})$ – a strategy consistent with conventional advancing-front techniques. While his algorithm maintains a Delaunay triangulation $\mathcal{T}$ = Del(X) of the current vertices, it is still fundamentally an advancing-front scheme – without guarantees on element shape quality. Rebay reported that his scheme produced very high-quality output in practice, typically outperforming conventional Delaunay-refinement techniques. Similar methods have been pursued by other authors, including Üngör and Erten, who, in [30], have shown that by carefully positioning refinement points on the Voronoi diagram, a set of generalised Steiner vertices for two-dimensional Delaunay-refinement can be realised. Üngör has shown that the theoretical guarantees associated with standard Delaunay-refinement techniques extend to such methods, offering the prospect of improved 'provably-good' mesh generation techniques. The use of so-called *generalised* off-centre Delaunay-refinement strategies has also been explored by Chernikov, Chrisochoides and Foteinos in [31,32], in which Steiner points are positioned within a set of *selection-balls* adjacent to element circumcentres. In [31], Chernikov and Chrisochoides show that a family of 'provably-good' generalised two- and three-dimensional Delaunay-refinement schemes exist, and can be realised via the specification of appropriate selection-ball radii parameters.

In this study, a generalisation of the ideas introduced by Rebay and Üngör is formulated for the three-dimensional meshing problem – using off-centre Steiner vertices to simulate the vertex placement strategy of an advancing-front approach, while maintaining the framework of a restricted Delaunay-refinement technique. The aim of such a strategy

Fig. 3. Off-centre Steiner points for surface refinement, showing (i) the surface ball associated with a 2-face $f \in \mathrm{Del}\,|_\Sigma(X)$, (ii) the plane $\mathcal{V}$ aligned with the local Voronoi face $v_f \in \mathrm{Vor}(X)$, (iii) placement of the size-optimal point $\mathbf{c}^{(2)}$ to satisfy local edge-length constraints.

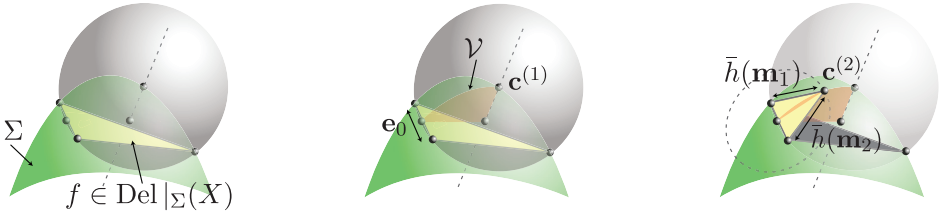

is to recover the high element quality and smooth point-placement behaviour generated by frontal methods, while inheriting the theoretical guarantees and robustness of Delaunay-refinement techniques. The new Frontal-Delaunay algorithm is an extension of the conventional restricted Delaunay-refinement algorithm presented in Section 2, modified to use 'off-centre' rather than circumcentre-based point-placement strategies. The set of constraints satisfied by the Frontal-Delaunay algorithm is identical to those incorporated in the restricted Delaunay-refinement scheme, with upper bounds on the radius-edge ratio $\bar{\rho}$, surface discretisation error $\bar{\epsilon}(\mathbf{x}_f)$, element size $\bar{h}(\mathbf{x}_f)$ and topological consistency all required to be satisfied for convergence. The Frontal-Delaunay scheme follows Algorithm 2.1.

3.2. Point-placement strategy (surface refinement)

The 'off-centre' point-placement strategy used to refine surface facets $f \in \mathrm{Del}\,|_\Sigma(X)$ is an evolution of the methods presented previously in [1,2] for surface mesh generation. Two candidate Steiner vertices are considered. Type I vertices, $\mathbf{c}^{(1)}$, are equivalent to conventional element circumcentres (positioned at the centre of the associated surface Delaunay balls), and are used to satisfy constraints on the element radius-edge ratios. Type II vertices, $\mathbf{c}^{(2)}$, are so-called *size-optimal* points, designed to satisfy element sizing constraints in a locally optimal fashion. Given a *refinable* 2-simplex $f \in \mathrm{Del}\,|_\Sigma(X)$, the Type II vertex $\mathbf{c}^{(2)}$ is positioned at an intersection of the surface Σ and a plane $\mathcal{V}$, where $\mathcal{V}$ is aligned with the local face of the Voronoi complex $v_f \in \mathrm{Vor}(X)$ associated with the short frontal edge $\mathbf{e}_0 \in f$. The vertex $\mathbf{c}^{(2)}$ is positioned such that it forms an isosceles triangle candidate σ about the frontal edge $\mathbf{e}_0$, such that its size $h(\sigma)$ satisfies local constraints. Specifically, the altitude of σ is computed from local mesh-size information, such that

$$a_\sigma = \min\Big(\big(\bar{h}_\sigma^2 - \|\tfrac{1}{2}\mathbf{e}_0\|^2\big)^{\frac{1}{2}},\ \sqrt{3}/2\,\bar{h}_\sigma\Big), \qquad \bar{h}_\sigma = \tfrac{1}{2}\big(\bar{h}(\mathbf{m}_1) + \bar{h}(\mathbf{m}_2)\big) \tag{1}$$

where the $\mathbf{m}_i$'s are the edge midpoints and $\sqrt{3}/2\,\bar{h}_\sigma$ is the altitude for an 'ideal' element. The position of the point $\mathbf{c}^{(2)}$ is calculated by computing the intersection of the surface Σ with a circle of radius a_σ, centred at the midpoint of the frontal edge $\mathbf{e}_0 \in f$ and inscribed on the plane $\mathcal{V}$. For non-uniform $\bar{h}(\mathbf{x})$, expressions for the position of the point $\mathbf{c}^{(2)}$ are weakly non-linear, and an iterative procedure is used to obtain an approximate solution. The positioning of size-optimal Type II Steiner vertices for surface facets is illustrated in Figure 3.

3.3. Point-placement strategy (volume refinement)

A similar point-placement strategy is employed for the refinement of tetrahedral elements, consisting of the placement of a pair of candidate Steiner vertices. Consistent with previous discussions, Type I vertices, $\mathbf{c}^{(1)}$, are equivalent to conventional element circumcentres, and are used to satisfy constraints on element radius-edge ratios. Type II vertices, $\mathbf{c}^{(2)}$, are designed to satisfy element sizing constraints in a locally optimal fashion. Given a *refinable* 3-simplex $\tau \in \mathrm{Del}\,|_\Omega(X)$, the Type II vertex $\mathbf{c}^{(2)}$ is positioned along the Voronoi edge segment $\mathbf{v}_f \in \mathrm{Vor}(X)$ associated with the small frontal 2-face $f_0 \in \tau$. The vertex $\mathbf{c}^{(2)}$ is positioned such that it forms an isosceles tetrahedron candidate σ about the frontal face $\mathbf{f}_0$, such that its size $h(\sigma)$ satisfies local mesh-size constraints. Given that $\mathrm{Del}\,|_\Omega(X)$ is Delaunay, a number of important properties regarding the Voronoi segment $\mathbf{v}_f$ are known, including, firstly, that $\mathbf{v}_f$ is orthogonal to f_0, and, secondly, that $\mathbf{v}_f$ passes through the centre of the diametric ball $\mathrm{B}(\mathbf{c}_0, r_0)$ associated with f_0. The altitude

Fig. 4. Placement of off-centre Steiner points in the volume Ω, showing (i) the local edge $v_e \in \mathrm{Vor}(X)$ of the Voronoi diagram associated with the small face $f_0 \in \tau$, and (ii) placement of the size-optimal vertex $\mathbf{c}^{(2)}$, such that local size constraints $\bar{h}(\mathbf{x}_\tau)$ are enforced.

(i) (ii)

of the tetrahedron σ is calculated using local mesh-size information, such that

$$a_\sigma = \min\Big(\big(\bar{h}_\sigma^2 - r_0^2\big)^{\frac{1}{2}},\ \sqrt{6}/3\,\bar{h}_\sigma\Big), \qquad \bar{h}_\sigma = \tfrac{1}{3}\Big(\bar{h}(\mathbf{m}_1) + \bar{h}(\mathbf{m}_2) + \bar{h}(\mathbf{m}_3)\Big) \tag{2}$$

where the $\mathbf{m}_i$'s are the edge midpoints and $\sqrt{6}/3\,\bar{h}_\sigma$ is the altitude for an 'ideal' element. The position of the point $\mathbf{c}^{(2)}$ is computed by projection along the vector $\mathbf{v}_f$, such that $\mathbf{c}^{(2)} = \mathbf{c}_0 + a_\sigma\,\hat{\mathbf{v}}$. An iterative procedure is used resolve the resulting non-linear expressions. The positioning of size-optimal Type II Steiner vertices for tetrahedral elements is illustrated in Figure 4.

3.4. Point-placement strategy (off-centre selection)

Given the Type I and Type II off-centres $\mathbf{c}^{(1)}$ and $\mathbf{c}^{(2)}$ for surface and volume elements, the positions of the associated refinement points $\mathbf{c}_f$ and $\mathbf{c}_\tau$ are calculated. These points are selected to satisfy the *limiting* local constraints, setting

$$\mathbf{c}_f = \begin{cases} \mathbf{c}_f^{(2)}, \text{ if } (d_f^{(2)} \le d_f^{(1)}) \text{ and } (d_f^{(2)} \ge \tfrac{1}{2}\|\mathbf{e}_0\|), \\ \mathbf{c}_f^{(1)}, \text{ otherwise} \end{cases} \quad \text{and} \quad \mathbf{c}_\tau = \begin{cases} \mathbf{c}_\tau^{(2)}, \text{ if } (d_\tau^{(2)} \le d_\tau^{(1)}) \text{ and } (d_\tau^{(2)} \ge r_0), \\ \mathbf{c}_\tau^{(1)}, \text{ otherwise} \end{cases} \tag{3}$$

where the $d^{(i)} = \|\mathbf{c}^{(i)} - \mathbf{c}_0\|$ are distances from the centre of the frontal facet to the Type I and Type II off-centres, respectively. This cascading selection criteria is designed to ensure that the refinement scheme smoothly degenerates to that of a conventional circumcentre-based Delaunay-refinement strategy in limiting cases, while using locally shape-optimal points where possible. Specifically, these constraints guarantee that the refinement points for both surface and volume elements lie within a 'safe' region – being positioned on an adjacent sub-face of the Voronoi complex and bound between the circumcentre of the element itself and the diametric ball of the associated frontal facet. Note that when element size is sufficiently small with respect to the local mesh-size function, the refinement points reduce to element circumcentres in all cases.

3.5. Refinement order

In addition to the use of 'off-centre' point-placement schemes, the Frontal-Delaunay algorithm also introduces changes to the order in which elements are refined. To better mimic the behaviour of an advancing-front type method, elements are refined only if they are adjacent to an existing 'frontal' entity. In the case of surface facets $f \in \mathrm{Del}\,|_\Sigma(X)$, the frontal edge $\mathbf{e}_0 \in f$ must be shared by at least one adjacent facet $f_j \in \mathrm{Del}\,|_\Sigma(X)$ that is 'converged' – satisfying its associated radius-edge, mesh-size and surface-error constraints. In the case of interior tetrahedral elements $\tau \in \mathrm{Del}\,|_\Omega(X)$, the frontal face $\mathbf{f}_0 \in \tau$ must either be a converged surface facet $f_j \in \mathrm{Del}\,|_\Sigma(X)$ or be shared by an adjacent tetrahedron $\tau_j \in \mathrm{Del}\,|_\Omega(X)$ that satisfies its associated radius-edge and mesh-size constraints. The idea of defining 'frontal' entities as a dynamic boundary between converged and un-converged elements in the mesh is a common feature of Frontal-Delaunay algorithms, with similar approaches presented in, for example, [26–29].

3.6. Convergence guarantees and robustness

The new off-centre point-placement schemes are derived by considering the fundamental properties associated with the underlying Voronoi diagram. Importantly, by constraining new Steiner vertices to lie along the sub-faces of $\mathrm{Vor}(X)$, it is guaranteed that the distribution of mesh vertices remains *well-separated* throughout the refinement process. This behaviour ensures that the algorithm does not create arbitrarily short edges. For the sake of brevity, a full proof of termination or correctness is not included here, but it is important to note that constraints on element radius-edge ratios $\rho(f)$, element size $h(\mathbf{x})$, surface discretisation error $\epsilon(f)$ and topological consistency are satisfied *by definition*, provided that termination of the algorithm is achieved in practice. The development of a suitable theoretical model for the new Frontal-Delaunay algorithm is the subject of a forthcoming publication.

4. Mesh-size functions

The construction of high-quality mesh-size functions is an important aspect of the restricted Delaunay-refinement and Frontal-Delaunay algorithms presented previously. A good mesh-size function $\bar{h}(\mathbf{x})$ incorporates sizing constraints imposed by both the user and the geometry of the domain to be meshed. The construction of high-quality mesh-size functions is a detailed process, and in-depth discussions are not presented here as a result. In this study, mesh-size estimates are computed using an approximation of the medial axis of the domain Ω, following the methods of Amenta et al. [33] and Dey and Zhao [34]. A smooth mesh-size function is subsequently obtained using a variation of the gradient-limiting approach of Persson [35]. Extended discussions, detailing the formation of high-quality mesh-size functions for three-dimensional domains are presented in [1,2].

5. Sliver suppression

Slivers are a class of low-quality tetrahedral elements that occur in three-dimensional Delaunay tessellations. Consisting of four vertices positioned in a thin 'kite'-like configuration, sliver elements are typically of very low shape-quality – possessing pathologically small dihedral angles, but relatively small radius-edge ratios. Due to these characteristics, sliver elements are typically not eliminated by standard Delaunay-based refinement schemes. Both the Delaunay-refinement and Frontal-Delaunay algorithms presented previously are susceptible to the generation of slivers. Various strategies designed to remove sliver elements are known to exist, including non-linear optimisation methods based on *sliver-exudation* [40] and *topological-optimisation* [41]. In this study, a simple method for the suppression of sliver elements is employed, in which slivers are eliminated through additional refinement. Following [36], any tetrahedron $\tau_i \in \mathrm{Del}\,|_\Omega(X)$ with a small *volume-length* ratio $v(\tau_i) \leq \bar{v}$ is marked for refinement, where $\bar{v}$ is a user-defined lower-bound on element volume-length ratios. Previous studies [36,37] have shown that this modified refinement algorithm is convergent for $\bar{v} \leq 1/3$. Noting that the volume-length ratio is a *robust* measure of element quality, known to detect all classes of low-quality tetrahedrons, the resulting meshes are of guaranteed quality, with bounded element dihedral angles and aspect ratios. Both the Delaunay-refinement and Frontal-Delaunay algorithms presented previously were modified to impose bounds on element volume-length ratios, meaning that both algorithms presented in this study satisfy bounds on (i) element radius-edge and volume-length ratios, (ii) element size, (iii) surface discretisation error, and (iv) topological consistency.

6. Results and discussion

The performance of the Delaunay-refinement and Frontal-Delaunay surface meshing algorithms presented in Sections 2 and 3 was investigated experimentally, with both techniques used to mesh a series of benchmark problems. Both the Frontal-Delaunay and Delaunay-refinement algorithms were implemented, allowing the performance and output of the two techniques to be compared side-by-side. Due to similarities in the overall algorithmic structure, a common code-base was used, with the algorithms differing only in the type of Steiner vertices inserted, as per the discussions outlined in Section 3. Care was taken to ensure that both methods were implemented in a consistent fashion, allowing unbiased comparisons to be made between the algorithms without needing to account for systemic

Fig. 5. Meshes for the ELEPHANT test-case, showing output for the JGSW-FD and CGAL-DR algorithms. Detailed mesh statistics are shown including normalised histograms of elements volume-length ratios, dihedral angles and relative edge-lengths. Element counts and total refinement times are also shown.

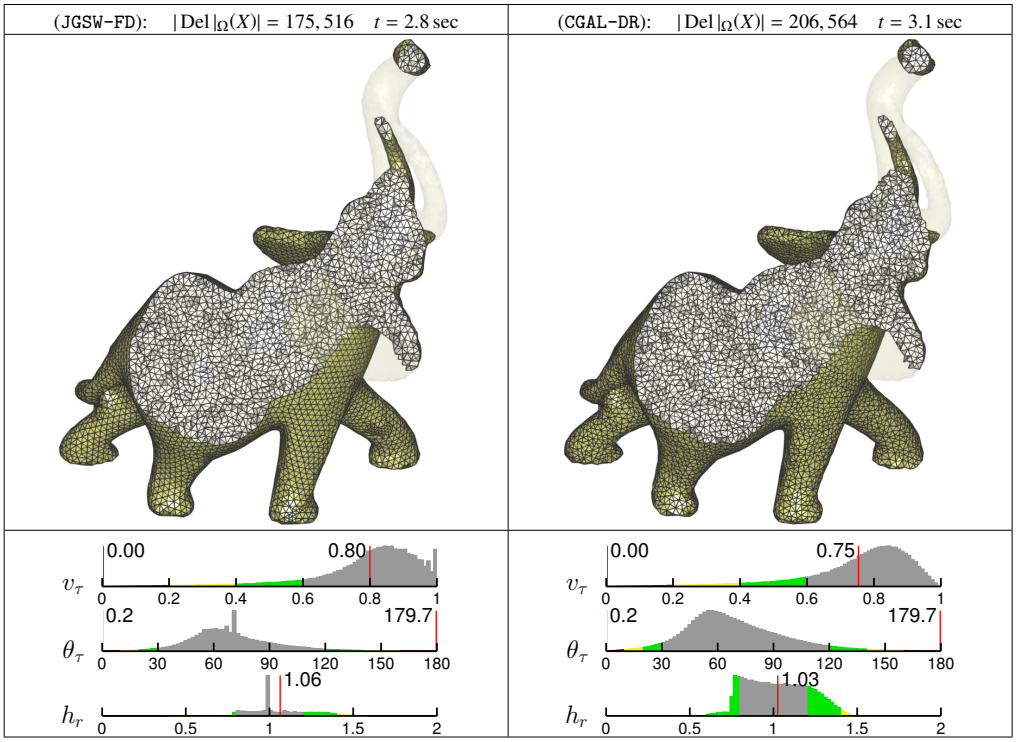

differences arising from particular implementation and/or design choices. Both algorithms were implemented in C++ and compiled as 64-bit executables. Both the Frontal-Delaunay and Delaunay-refinement algorithms have been implemented as part of the JIGSAW meshing package, currently available by request from the author. These implementations are referred to as JGSW-FD and JGSW-DR throughout, with the suffixes -FD and -DR denoting the 'Frontal-Delaunay' and 'Delaunay-refinement' variants, respectively.

In order to provide additional performance information, the well-known CGALMESH implementation [16] was also included in a subset of the meshing comparisons. The CGALMESH algorithm was sourced from version 4.6 of the CGAL package [38,39] and was compiled as a 64-bit library. The CGALMESH algorithm is referred to as CGAL-DR throughout the following discussions, with the suffix -DR denoting 'Delaunay-refinement'. All tests were run using a single core of an Intel i7 processor. Visualisation and post-processing was completed using MATLAB.

6.1. Preliminaries

The various Delaunay-refinement and Frontal-Delaunay algorithms were used to mesh a pair of benchmark problems, including (i) a generic test-case presented in Figure 5, in which the performance of the new JGSW-FD algorithm and the existing CGAL-DR implementation was compared, (ii) an additional biomedical test-case shown in Figure 6, designed to contrast the performance of the JGSW-FD and JGSW-DR algorithms.

In all test cases, constant radius-edge ratio thresholds were specified for both surface and volume elements, such that $\bar{\rho}_f = 1$ and $\bar{\rho}_\tau = 2$, corresponding to $\theta_{\min} \geq 30^\circ$ for surface facets. Additionally, non-uniform surface discretisation constraints were enforced, setting $\bar{\epsilon}(\mathbf{x}) = \beta\bar{h}(\mathbf{x})$, with $\beta = 1/4$.

For all test problems, detailed statistics on element quality are presented, including histograms of element *volume-length* ratios $v(\tau)$, *dihedral-angles* $\theta(\tau)$, and *relative edge-length* $\bar{h}_r$. The element volume-length ratio is a robust measures of element quality, where high-quality elements attain scores that approach unity. The relative edge-length

is defined to be the ratio of edge-length $\|\mathbf{e}\|$ to desired edge-length $\bar{h}(\mathbf{x}_e)$, where $\mathbf{x}_e$ is the edge midpoint. Relative edge-lengths close to unity indicate conformance to the mesh-size function. High-quality surface triangles contain angles of 60.0°, while high-quality tetrahedrons contain angles approaching 70.5°. Histograms further highlight the minimum, maximum and mean values of the relevant distributions as appropriate.

6.2. A Comparison of JGSW-FD and CGAL-DR

The performance of the JGSW-FD and CGAL-DR algorithms was assessed using the generic ELEPHANT test-case. Meshes were generated using uniform mesh-size constraints, with a small constant value, $\bar{h}(\mathbf{x}) = \alpha$, imposed globally, where α was chosen to be approximately 2% of the mean bounding-box dimension associated with the model. Due to differences in the way that mesh-size constraints are interpreted by the two meshing packages, the mesh-size value selected for the CGAL-DR algorithm was reduced by a factor of $4/3$. This reduction accounts for the fact that in CGAL-DR, mesh-size constraints are imposed with respect to the element circumradii, whereas the JGSW-FD algorithm treats the mesh-size function in terms of element edge length. Both algorithms were found to produce meshes incorporating consistent mean edge-lengths based on these modified mesh-size values. The CGAL-DR package does not support the option to detect and refine sliver elements via additional refinement, so a volume-length threshold $\bar{\nu} = 0$ was imposed to allow a fair comparison. Use of the non-linear sliver exudation and optimisation routines provided by the CGAL package is beyond the scope of this paper.

The results in Figure 5 show that, overall, the new JGSW-FD algorithm generates a smaller mesh with improved element quality characteristics and mesh-size conformance when compared to the CGAL-DR algorithm. Overall computational expense for both algorithms was found to be similar. In terms of element counts, the new method leads to a reduction of approximately 15%. Focusing on the distribution of element shape-quality explicitly, it can be seen that the JGSW-FD algorithm achieves moderate improvements in mean volume-length and dihedral-angle distributions, with a subset of very high-quality elements ($\nu_\tau \simeq 1$, $\theta_\tau \simeq 70°$) generated. Comparisons of distributions of element relative-length reveal the largest differences, with the JGSW-FD algorithm showing significantly improved conformance to the imposed mesh-size function, with a tight clustering of h_r about 1. This result is not unexpected – confirming that the new size-optimal off-centre point-placement scheme leads to high-quality vertex distributions that follow the imposed sizing distribution. Recalling that $\bar{\nu} = 0$ in this test, meshes generated by both algorithms are seen to contain a small number of low-quality sliver elements.

6.3. A Comparison of JGSW-FD and JGSW-DR

The performance of the JGSW-FD and JGSW-DR algorithms is next examined. While CGAL-DR and JGSW-DR are representative of the same class of meshing *algorithms*, the benchmarks included in this section allow for an unbiased comparison of the Frontal-Delaunay and Delaunay-refinement approaches, with both the JGSW-FD and JGSW-DR algorithms benefiting from the same set of implementation design and optimisation decisions.

Meshes for the FOOT test-case were generated using uniform mesh-size constraints, with a small constant value, $\bar{h}(\mathbf{x}) = \alpha$, imposed globally, where α was chosen to be approximately 1% of the mean bounding-box dimension associated with the model. Volume-length driven refinement was also used to eliminate low-quality sliver elements, with $\bar{\nu} = 0.1$ imposed for both algorithms.

Consistent with previous results, Figure 6 shows that, overall, the new JGSW-FD algorithm generates a smaller mesh with improved element quality characteristics and mesh-size conformance when compared to the JGSW-DR algorithm. Use of the JGSW-FD algorithm is seen to reduce elements counts by approximately 8%. As per previous analyses, the JGSW-FD algorithm is seen to achieve moderate improvements in mean volume-length and dihedral-angle distributions, but significant improvements in terms of mesh-size conformance. Meshes produced by both algorithms are seen to be free of low-quality sliver elements, with dihedral angles bounded above approximately 5° and below 170°. These results confirm the effective use of volume-length driven refinement to suppress slivers.

7. Conclusions

A new Frontal-Delaunay meshing algorithm has been developed to generate Delaunay meshes for three-dimensional domains bounded by smooth 2-manifold surfaces. The new algorithm is based on the so-called *restricted* Delaunay

Fig. 6. Meshes for the FOOT test-case, showing output for the JGSW-FD and JGSW-DR algorithms. Detailed mesh statistics are shown including normalised histograms of elements volume-length ratios, dihedral angles and relative edge-lengths. Element counts and total refinement times are also shown.

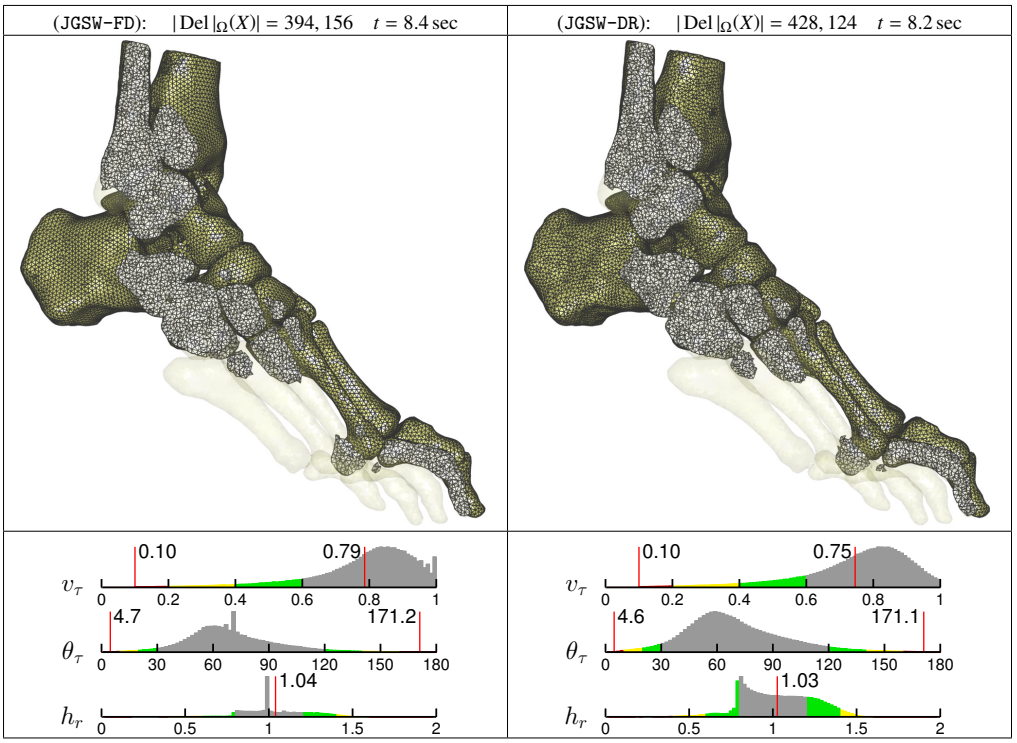

paradigm, in which a surface triangulation Del $|_\Sigma(X)$, and a volume mesh Del $|_\Omega(X)$ is constructed as a subset of a full-dimensional Delaunay tessellation Del(X). Through the introduction of new Voronoi-type off-centre point-placement schemes for the refinement of surface and volume elements, the new Frontal-Delaunay algorithm has been shown to combine the advantages of conventional advancing-front and Delaunay-refinement techniques. Specifically, it has been shown that this new hybrid approach allows for the insertion of both shape- and size-optimal Steiner points, and that the resulting surface and volume meshes are of very high-quality. It has been demonstrated that the new algorithm outperforms conventional Delaunay-refinement techniques, generating meshes of reduced size and with improved quality and grading statistics. Importantly, it has also been demonstrated that the new Frontal-Delaunay algorithm satisfies the same set of constraints as conventional Delaunay-refinement approaches, adhering to limits on element radius-edge ratios, mesh-size, surface discretisation error and mesh topology. It is expected that applications that place a premium on high mesh-quality, including problems in computational fluid dynamics and/or structural analysis, may benefit from the new Frontal-Delaunay technique. Future work will focus on providing support for an extended class of geometry representations, including domains containing sharp features.

Acknowledgements. This work was conducted at the University of Sydney with the support of an Australian Postgraduate Award. The author wishes to thank the anonymous reviewers for their helpful comments and feedback.

References

[1] D. Engwirda, D. Ivers, Face-centred Voronoi refinement for surface mesh generation, Procedia Engineering 82 (2014) 8–20.
[2] D. Engwirda, D. Ivers, Size-optimal Steiner points for Delaunay-refinement on curved surfaces, arXiv preprint arXiv:1501.04002 (2015).
[3] J. Peraire, J. Peiró, K. Morgan, Advancing-Front Grid Generation, in: J. F. Thompson, B. K. Soni, N. P. Weatherill (Eds.), Handbook of Grid Generation, Taylor & Francis, 1998. URL: http://books.google.com.au/books?id=ImaDT6ijKq4C.

[4] J. Schöberl, NETGEN: An Advancing Front 2D/3D Mesh Generator based on Abstract Rules, Computing and Visualization in Science 1 (1997) 41–52.
[5] D. Rypl, Approaches to Discretization of 3D Surfaces, in: CTU Reports, volume 7, CTU Publishing House, Prague, Czech Republic, 2003.
[6] J. Schreiner, C. E. Scheidegger, S. Fleishman, C. T. Silva, Direct (Re)Meshing for Efficient Surface Processing, Computer Graphics Forum 25 (2006) 527–536.
[7] L. P. Chew, Guaranteed-quality Triangular Meshes, Technical Report, Cornell University, Department of Computer Science, Ithaca, New York, 1989.
[8] J. Ruppert, A New and Simple Algorithm for Quality 2-dimensional Mesh Generation, in: Proceedings of the fourth annual ACM-SIAM Symposium on Discrete algorithms, SODA '93, 1993, pp. 83–92.
[9] A Delaunay Refinement Algorithm for Quality 2-Dimensional Mesh Generation, Journal of Algorithms 18 (1995) 548 – 585.
[10] J. R. Shewchuk, Delaunay Refinement Mesh Generation, Ph.D. thesis, Pittsburg, Pennsylvania, 1997.
[11] J. R. Shewchuk, Tetrahedral Mesh Generation by Delaunay Refinement, in: Proceedings of the fourteenth annual symposium on Computational geometry, SCG '98, ACM, New York, NY, USA, 1998, pp. 86–95. doi:10.1145/276884.276894.
[12] S. Cheng, T. Dey, Quality Meshing with Weighted Delaunay Refinement, SIAM Journal on Computing 33 (2003) 69–93.
[13] S. W. Cheng, T. K. Dey, E. A. Ramos, Delaunay Refinement for Piecewise Smooth Complexes, Discrete & Computational Geometry 43 (2010) 121–166.
[14] J. D. Boissonnat, S. Oudot, Provably Good Surface Sampling and Approximation, in: ACM International Conference Proceeding Series, volume 43, 2003, pp. 9–18.
[15] J. D. Boissonnat, S. Oudot, Provably Good Sampling and Meshing of Surfaces, Graphical Models 67 (2005) 405–451.
[16] C. Jamin, P. Alliez, M. Yvinec, J. D. Boissonnat, CGALmesh: A Generic Framework for Delaunay Mesh Generation, Technical Report, INRIA, 2013.
[17] H. Edelsbrunner, N. R. Shah, Triangulating Topological Spaces, International Journal of Computational Geometry & Applications 7 (1997) 365–378.
[18] S. W. Cheng, T. K. Dey, J. R. Shewchuk, Delauay Mesh Generation, Taylor & Francis, New York, 2013.
[19] J. R. Shewchuk, General-dimensional Constrained Delaunay and Constrained Regular Triangulations, I: Combinatorial Properties, Discrete & Computational Geometry 39 (2008) 580–637.
[20] H. Si, Adaptive Tetrahedral Mesh Generation by Constrained Delaunay Refinement, International Journal for Numerical Methods in Engineering 75 (2008) 856–880.
[21] S. W. Cheng, T. K. Dey, J. A. Levine, A Practical Delaunay Meshing Algorithm for a Large Class of Domains, in: Proceedings of the 16th international meshing roundtable, Springer, 2008, pp. 477–494.
[22] S. Oudot, L. Rineau, M. Yvinec, Meshing Volumes Bounded by Smooth Surfaces, in: Proceedings of the 14th International Meshing Roundtable, Springer, 2005, pp. 203–219.
[23] A. Bowyer, Computing Dirichlet Tessellations, The Computer Journal 24 (1981) 162–166.
[24] P. Alliez, S. Tayeb, C. Wormser, AABB Tree, Technical Report, 2009.
[25] H. Erten, A. Üngör, Quality Triangulations with Locally Optimal Steiner Points, SIAM J. Sci. Comp. 31 (2009) 2103–2130.
[26] S. Rebay, Efficient Unstructured Mesh Generation by Means of Delaunay Triangulation and Bowyer-Watson Algorithm, Journal of Computational Physics 106 (1993) 125 – 138.
[27] D. J. Mavriplis, An Advancing Front Delaunay Triangulation Algorithm Designed for Robustness, Journal of Computational Physics 117 (1995) 90 – 101.
[28] P. J. Frey, H. Borouchaki, P. L. George, 3D Delaunay Mesh Generation Coupled with an Advancing-Front Approach, Computer Methods in Applied Mechanics and Engineering 157 (1998) 115 – 131.
[29] J. F. Remacle, F. Henrotte, T. Carrier-Baudouin, E. Béchet, E. Marchandise, C. Geuzaine, T. Mouton, A Frontal-Delaunay Quad-Mesh Generator using the $\mathbb{L}^\infty$-norm, International Journal for Numerical Methods in Engineering 94 (2013) 494–512.
[30] A. Üngör, Off-centers: A New Type of Steiner Points for Computing Size-optimal Guaranteed-quality Delaunay Triangulations, Computational Geometry: Theory and Applications 42 (2009) 109–118.
[31] A. N. Chernikov, N. P. Chrisochoides, Generalized insertion region guides for delaunay mesh refinement, SIAM Journal on Scientific Computing 34 (2012) A1333–A1350.
[32] P. A. Foteinos, A. N. Chernikov, N. P. Chrisochoides, Fully generalized two-dimensional constrained delaunay mesh refinement, SIAM Journal on Scientific Computing 32 (2010) 2659–2686.
[33] N. Amenta, S. Choi, R. K. Kolluri, The power crust, unions of balls, and the medial axis transform, Computational Geometry 19 (2001) 127–153.
[34] T. K. Dey, W. Zhao, Approximating the medial axis from the Voronoi diagram with a convergence guarantee, Algorithmica 38 (2004) 179–200.
[35] P.-O. Persson, Mesh Size Functions for Implicit Geometries and PDE-based Gradient Limiting, Engineering with Computers 22 (2006) 95–109.
[36] S. Gosselin, C. Ollivier-Gooch, Tetrahedral Mesh Generation using Delaunay Refinement with Non-standard Quality Measures, International Journal for Numerical Methods in Engineering 87 (2011) 795–820.
[37] D. Engwirda, Locally optimal Delaunay-refinement and optimisation-based mesh generation, Ph.D. thesis, 2014.
[38] C. Jamin, S. Pion, M. Teillaud, 3D Triangulations, in: CGAL User and Reference Manual, 4.6.1 ed., CGAL Editorial Board, 2015.
[39] C. Jamin, S. Pion, M. Teillaud, 3D Triangulation Data Structure, in: CGAL User and Reference Manual, 4.6.1 ed., CGAL Editorial Board, 2015.
[40] S. W. Cheng, T. K. Dey, H. Edelsbrunner, M. A. Facello, S. H. Teng, Silver Exudation, J. ACM 47 (2000) 883–904.
[41] B. M. Klingner, J. R. Shewchuk, Aggressive Tetrahedral Mesh Improvement, in: M. L. Brewer, D. Marcum (Eds.), Proceedings of the 16th International Meshing Roundtable, Springer Berlin Heidelberg, 2008, pp. 3–23. doi:10.1007/978-3-540-75103-8_1.